

Top-quark and jet production in post CT18 PDF analyses

Marco Guzzi

Kennesaw State University

with

A. Ablat, K. Xie, S. Dulat, T.-J. Hou,

I. Sitiwaldi, and C.-P. Yuan

2307.11153 [hep-ph]



KENNESAW STATE
UNIVERSITY

Main Goals

Work is going on towards the upcoming release of CTEQ PDFs: CT2X ($X>2$).

- Efforts are being put into:
 1. selecting the most sensitive data from recent high-precision measurements at the LHC.
 2. understanding uncertainties and their intricacies in a multitude of scattering processes entering the global analysis (e.g., scale uncertainties).
- This talk: focuses on eligible $t\bar{t}$ production measurements at the LHC 13 TeV and their impact on the gluon PDF at large x from an optimal baseline selection of measurements of 1D absolute differential Xsec. [2307.11153 \[hep-ph\]](#)

Motivations

- Assess the impact of new $t\bar{t}$ production 1D diff. Xsec measurements on unpol. coll. PDFs
- Improve PDF uncertainties in global QCD analyses (in particular, $g(x)$ at large x)
- Explore QCD dynamics and interplay between jet and $t\bar{t}$ production in PDFs at large x

Important for: precision BSM searches, precise and accurate theory predictions (pQCD),...

Challenges:

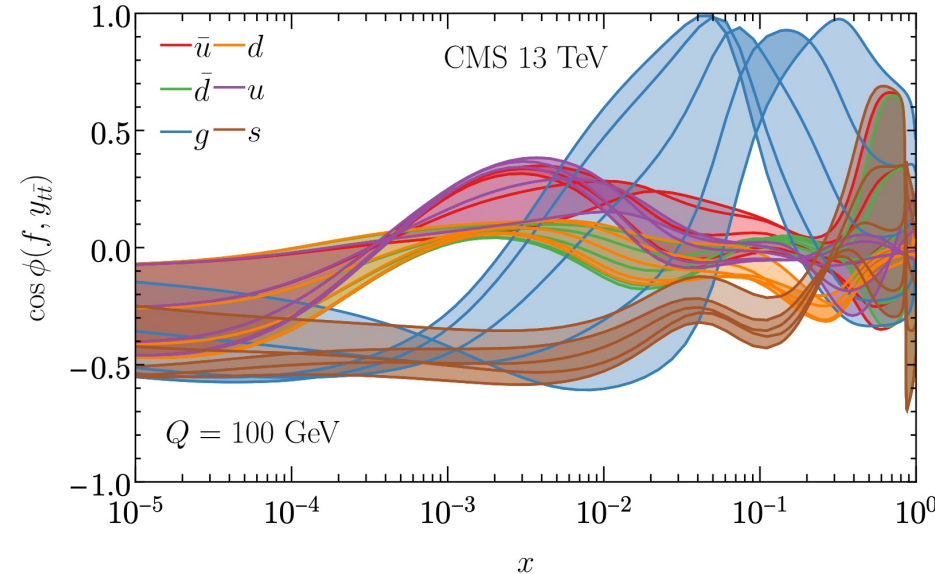
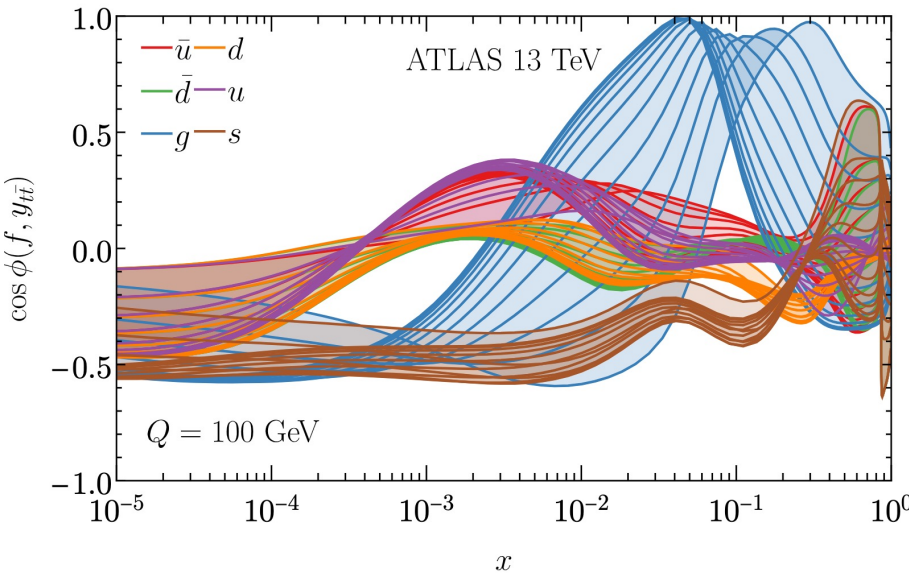
- Compatibility between various top-quark data in the post CT18 global fit
- Treatment of correlated systematic unc. and statistical correlations

What are data telling us?

- Heavy-quark production at the LHC at small p_T and large rapidity y of the heavy quark: sensitive to PDFs at both small and large x (especially true for c/b production)

$$x_{1,2} \approx \frac{\sqrt{p_T^2 + m_Q^2}}{\sqrt{S}} e^{\pm y}$$

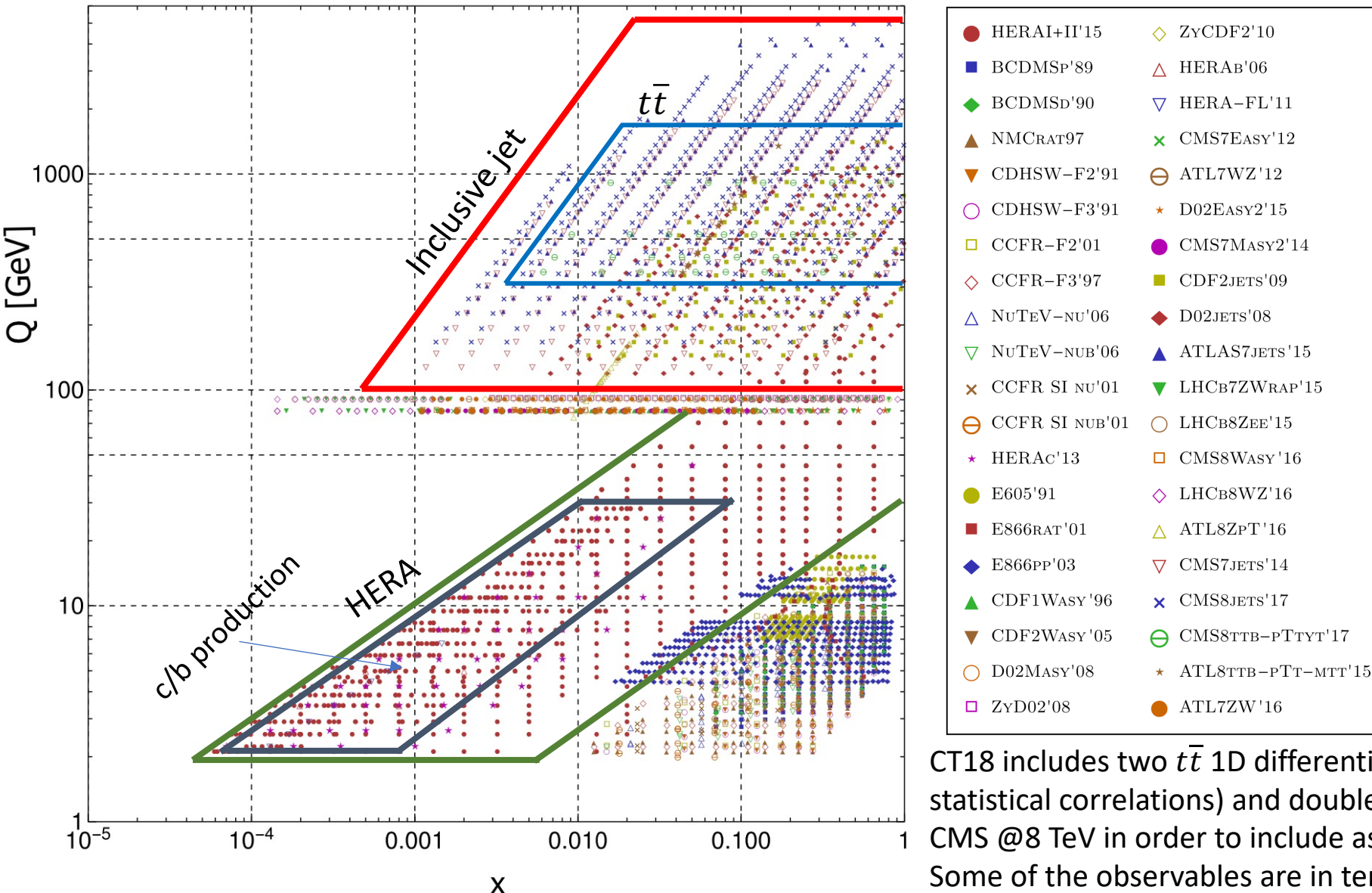
- In this kinematic region PDFs are poorly constrained by other experiments in global PDF fits.
- Top-quark pair production @LHC can already probe the gluon PDF at $x \gtrsim 0.01$



Correlation plots with ePump for the ATLAS all-hadronic and CMS dilepton channel

PDF Kinematics in the Q - x plane and the CT18 fit

Experimental data in CT18 PDF analysis



Jet and $t\bar{t}$ complement each other in the kinematic plane. They impact the gluon PDF at large x . Important to disentangle the effect due to jet production and top-quark data.

Top and jet Data in CT18

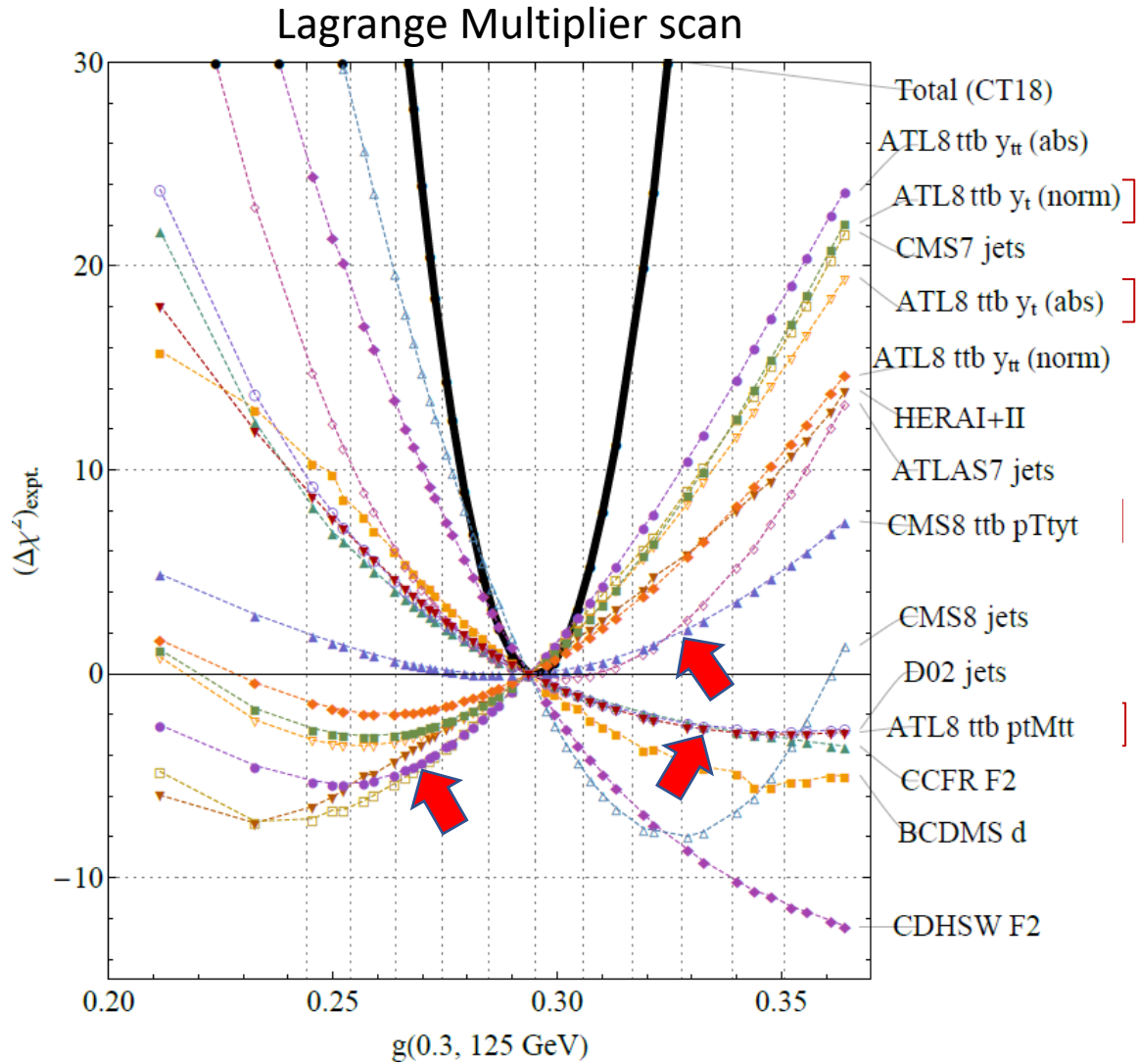
Top-quark
1511.04716 ATLAS 8 TeV tt b ptT diff. distributions
1511.04716 ATLAS 8 TeV tt b mtt diff. distributions
1703.01630 CMS 8 TeV tt b (pT, yt) 2d diff. distrib.

Jet production
1406.0324 CMS incl. jet at 7 TeV with R=0.7
1410.8857 ATLAS incl. jet at 7 TeV with R=0.6
1609.05331 CMS incl. jet at 8 TeV with R=0.7

CT18 includes two $t\bar{t}$ 1D differential observables from ATLAS (using statistical correlations) and double differential measurements from CMS @8 TeV in order to include as much information as possible.
Some of the observables are in tension with each other.

Constraints from 8 TeV $t\bar{t}$ production data in CT18

CT18 NNLO + unfitted ATLAS 8 TeV top single-diff. data



Realistic PDF error estimates account for multiple PDF functional forms and some disagreements between the measurements.

They predict milder impact from $t\bar{t}$ data

In the figure, pulls on the gluon from ATLAS8 $y_{t\bar{t}}$ and y_t distributions (absolute or normalized) agree with HERA DIS, oppose ATLAS8 $d^2\sigma/(dp_{T,t} dm_{t\bar{t}})$ and CMS8 $d^2\sigma/(dp_{T,t} dy_{t,\text{ave}})$

Impact of LHC 13 TeV $t\bar{t}$ production on CT2X PDFs

| Exp | Obs | N_{pt} | ePump | | Global fit | | |
|--|---|-----------------|-------|---------|------------|---------|---------|
| | | | H_T | $H_T/2$ | $H_T/4$ | $H_T/2$ | $H_T/4$ |
| ATL13had | $m_{t\bar{t}}$ | 9 | 1.75 | 1.57 | 1.60 | 1.53 | 1.47 |
| | $H_T^{t\bar{t}}$ | 11 | 1.98 | 1.77 | 1.59 | 1.50 | 1.74 |
| | $y_{t\bar{t}}$ | 12 | 1.28 | 1.15 | 0.94 | 1.05 | 1.07 |
| | p_{T,t_1} | 10 | 1.30 | 1.19 | 1.12 | 1.20 | 1.33 |
| | p_{T,t_2} | 8 | 1.13 | 0.84 | 1.05 | 0.84 | 1.59 |
| CMS13ll | $m_{t\bar{t}}$ | 7 | 3.46 | 3.07 | 3.14 | 3.12 | 3.23 |
| | $y_{t\bar{t}}$ | 10 | 1.66 | 0.97 | 0.68 | 0.94 | 0.67 |
| | $p_{T,t}$ | 6 | 3.60 | 3.70 | 3.68 | 3.56 | 3.05 |
| | y_t | 10 | 1.33 | 0.94 | 0.87 | 1.00 | 0.69 |
| CMS13lj | $m_{t\bar{t}}$ | 15 | 1.49 | 1.38 | 1.81 | 1.20 | 1.67 |
| | $y_{t\bar{t}}$ | 10 | 6.47 | 6.24 | 6.42 | 6.01 | 5.88 |
| CMS bins | | | | | | | |
| | $m_{t\bar{t}}$ | 7 | 2.40 | 1.17 | 0.68 | 0.83 | 0.66 |
| | $y_{t\bar{t}}$ | 10 | 0.91 | 0.69 | 0.62 | 0.74 | 0.75 |
| | $p_{T,t}$ | 6 | 2.34 | 2.01 | 2.47 | 1.35 | 1.43 |
| | y_t | 10 | 1.30 | 1.07 | 1.10 | 1.16 | 0.68 |
| ATLAS bins without statistical correlation (NSC) | | | | | | | |
| ATL13lj | $m_{t\bar{t}}$ | 9 | 1.55 | 1.12 | 0.94 | 1.27 | 0.92 |
| | $y_{t\bar{t}}$ | 7 | 0.91 | 0.74 | 0.80 | 0.76 | 0.90 |
| | $y_{t\bar{t}}^B$ | 9 | 1.40 | 1.27 | 1.53 | 0.85 | 0.93 |
| | $H_T^{t\bar{t}}$ | 9 | 1.35 | 0.91 | 0.93 | 0.81 | 0.80 |
| | $m_{t\bar{t}} + y_{t\bar{t}} + y_{t\bar{t}}^B + H_T^{t\bar{t}}$ | 34 | 1.87 | 1.28 | 1.46 | 0.93 | 1.06 |
| ATLAS bins with statistical correlations (WSC) | | | | | | | |
| | $m_{t\bar{t}}$ | 9 | 1.68 | 1.35 | 0.98 | 1.29 | 0.96 |
| | $y_{t\bar{t}}$ | 7 | 0.88 | 0.75 | 0.92 | 0.75 | 0.92 |
| | $y_{t\bar{t}}^B$ | 9 | 1.06 | 0.87 | 1.01 | 0.86 | 0.99 |
| | $H_T^{t\bar{t}}$ | 9 | 1.40 | 0.85 | 0.85 | 0.86 | 0.86 |
| | $m_{t\bar{t}} + y_{t\bar{t}} + y_{t\bar{t}}^B + H_T^{t\bar{t}}$ | 34 | 3.10 | 1.61 | 1.32 | 1.59 | 1.32 |

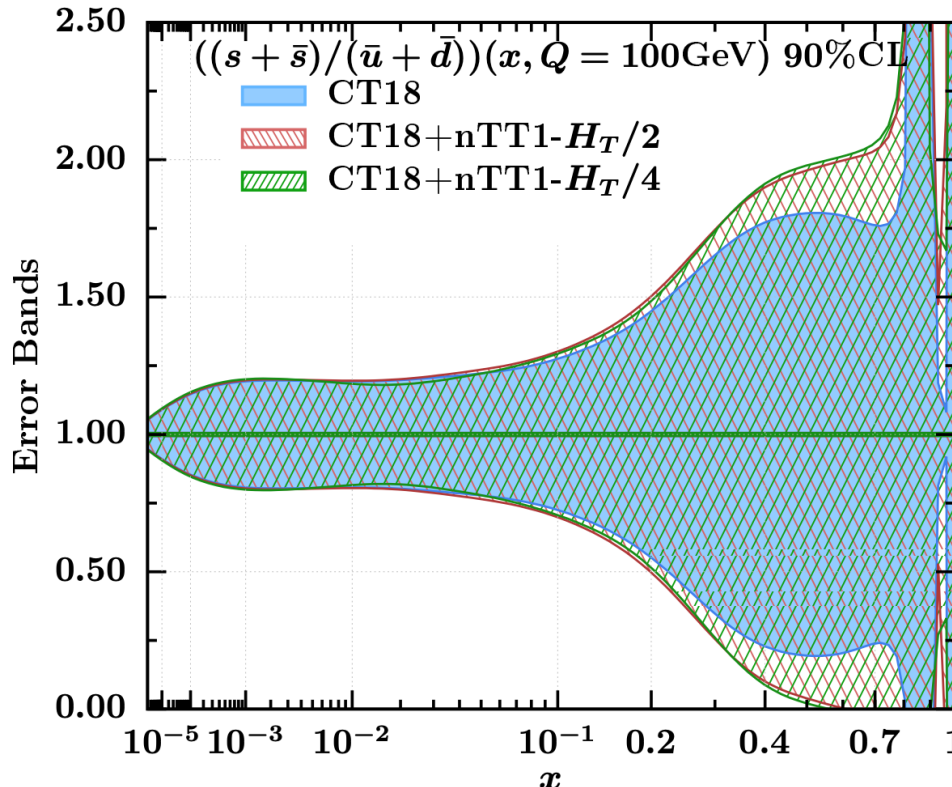
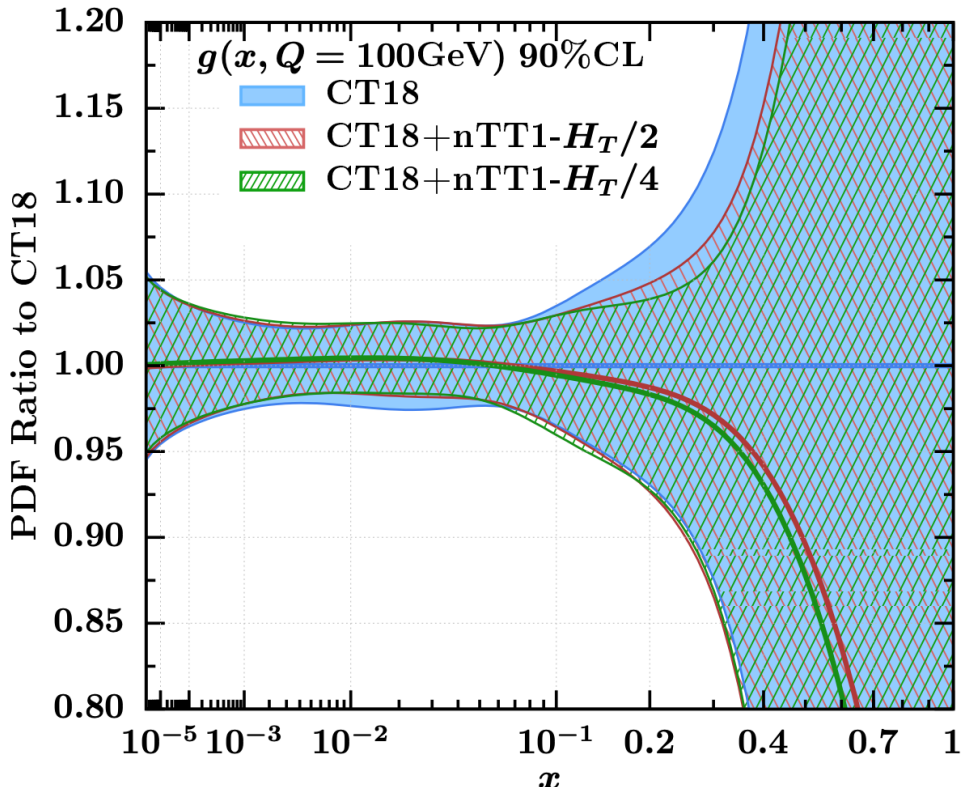
Extensive analysis in which the impact of 1D absolute distributions is explored with different scale choices

CT2X ⊇ CT18 + new optimal combination of top-quark pair production @LHC13 TeV from:

- ATLAS all hadronic, JHEP 01 (2021) 033, arXiv:2006.09274
- ATLAS lepton + jets, EPJC 79 (2019) 1028, arXiv:1908.07305
- CMS dilepton, JHEP 1902 (2019) 149, arXiv:1811.06625
- CMS lepton + jets, PRD 104 092013 (2021), arXiv:2108.02803

Correlated Systematic Uncertainties: ATLAS -> nuisance parameters
CMS -> Covariance matrix representation
When statistical correlations not provided → data added one at a time on top of the CT18 baseline

Global fit: impact from new baseline and μ -scale



Theory predictions:

- **MATRIX** (Catani, Grazzini et al. PRD 2019)
- **FastNNLO** (Czakon, et al. 1704.08551)

Blue band: CT18NNLO 90% C.L.
Hatched bands: CT18+new-data
Green: $\mu_R = \mu_F = H_T/2$
Red: $\mu_R = \mu_F = H_T/4$

Differences related to different scale choices are well within the CT18 PDF error band.

Optimal baselines consist of combinations of 1D absolute Xsec from



- ATLAS all hadronic, ytt
- ATLAS lepton + jets, ytt and stat. comb. {ytt, Mtt, yBtt, HTtt} have very similar impact
- CMS dilepton, ytt
- CMS lepton + jets, Mtt

Theory calculation setup

- CMS (dilepton ch): FastNLO grids for the NNLO theory– ([Czakon et al. 1704.08551](#))
- ATLAS: bin-by-bin NNLO/NLO K-factors generated by MATRIX ([Catani, Grazzini, et al. PRD2019](#))

The NLO QCD calculation is obtained using our in-house APPLGrid fast tables ([Carli et al. EPJC 2010](#)) generated with MCFM ([Campbell, Ellis JPG 2015](#))

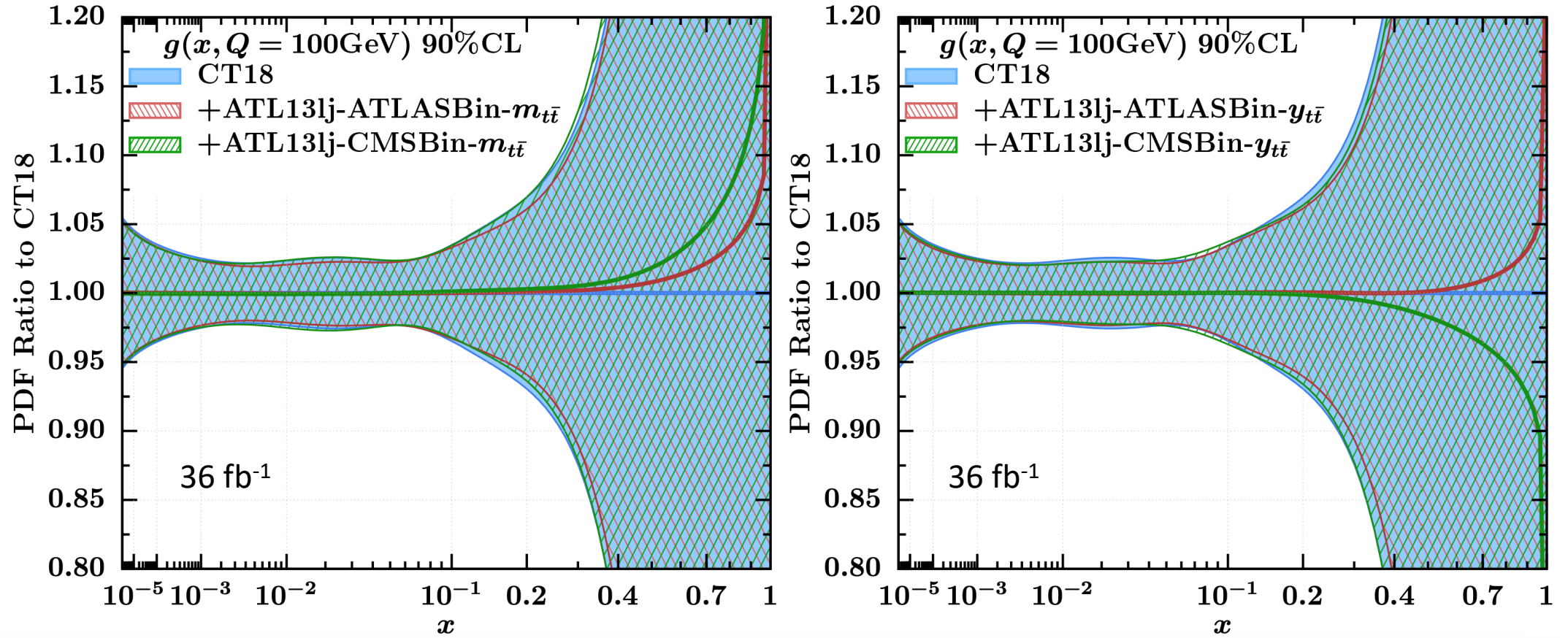
- m_t (pole) = 172.5 GeV
- Fact/Ren scale choice:

$m_{tt}, p_{T,tt}, y_{tt}, y_t$ use: $H_T/4$ and $H_T/2$; $p_{T,t}$, use M_T ; $p_{T,t} \text{ avg}$ use $M_T/2$ ([Czakon et al. JHEP 2017](#))

$$\mu_F = \mu_R = H_T/4 = \left(\sqrt{m_t^2 + p_{T,t}^2} + \sqrt{m_t^2 + p_{T,\bar{t}}^2} \right) / 4 \quad \mu_{F,R} = M_T^t/2 = \sqrt{m_t^2 + p_T^2}/2$$

- **EW corrections considered:** negligible impact on our fits.

Global fit: Impact on $g(x, Q)$ from ATLAS lep+jets

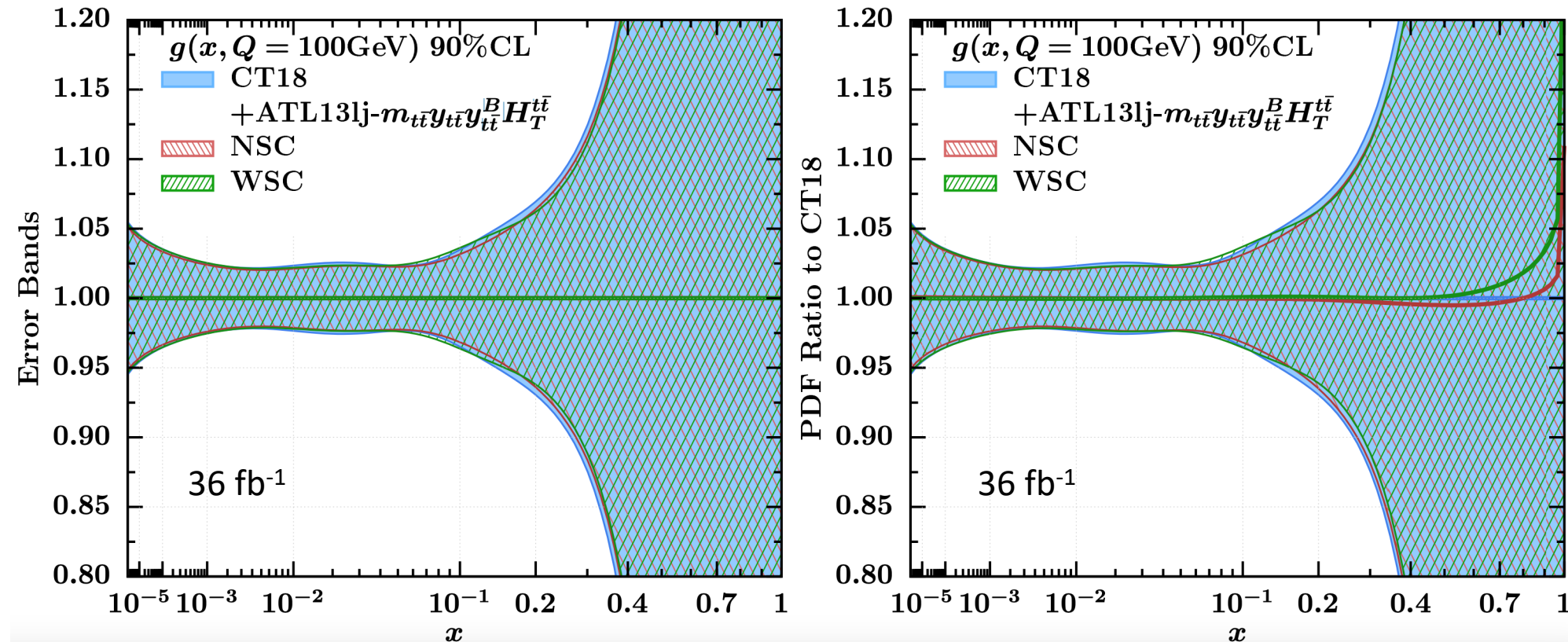


$M_{t\bar{t}}$ and $y_{t\bar{t}}$ 1D absolute distributions added one by one in the global fit.

Different results when different binning for the same distr. are used

Pulls are not in the same direction. $M_{t\bar{t}}$ badly described in terms of χ^2/N_{pt} . We select $y_{t\bar{t}}$ 1D absolute

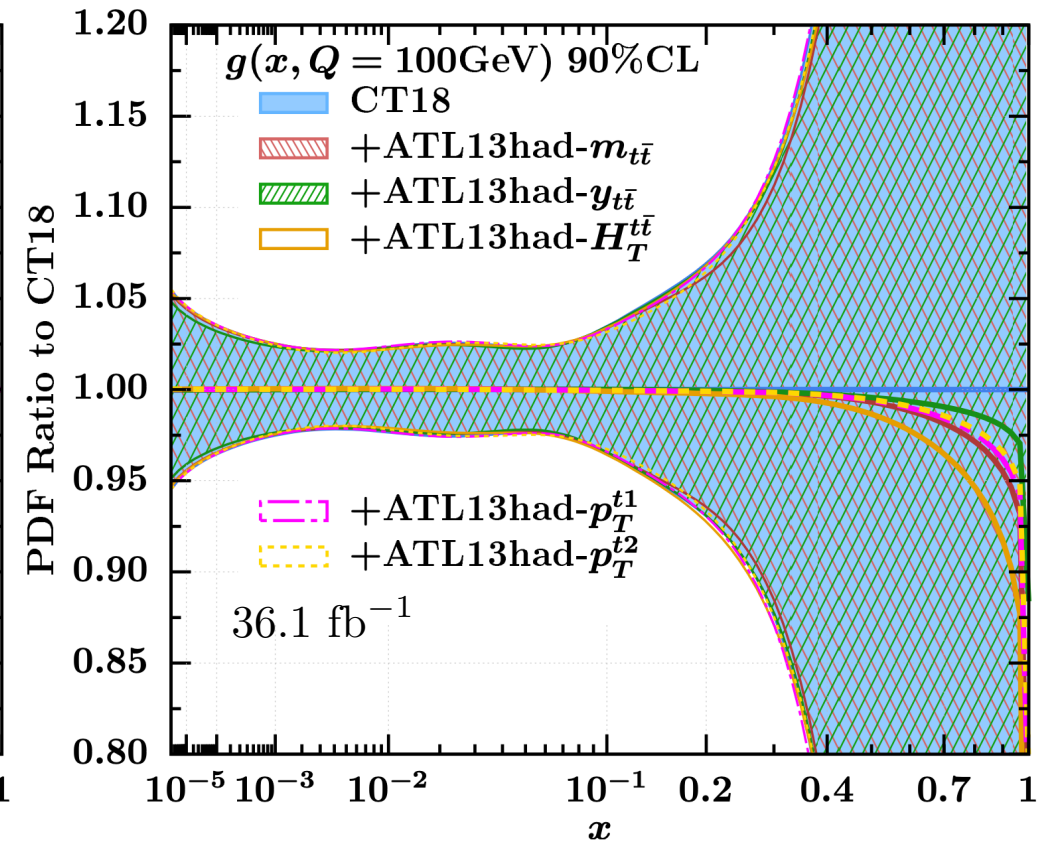
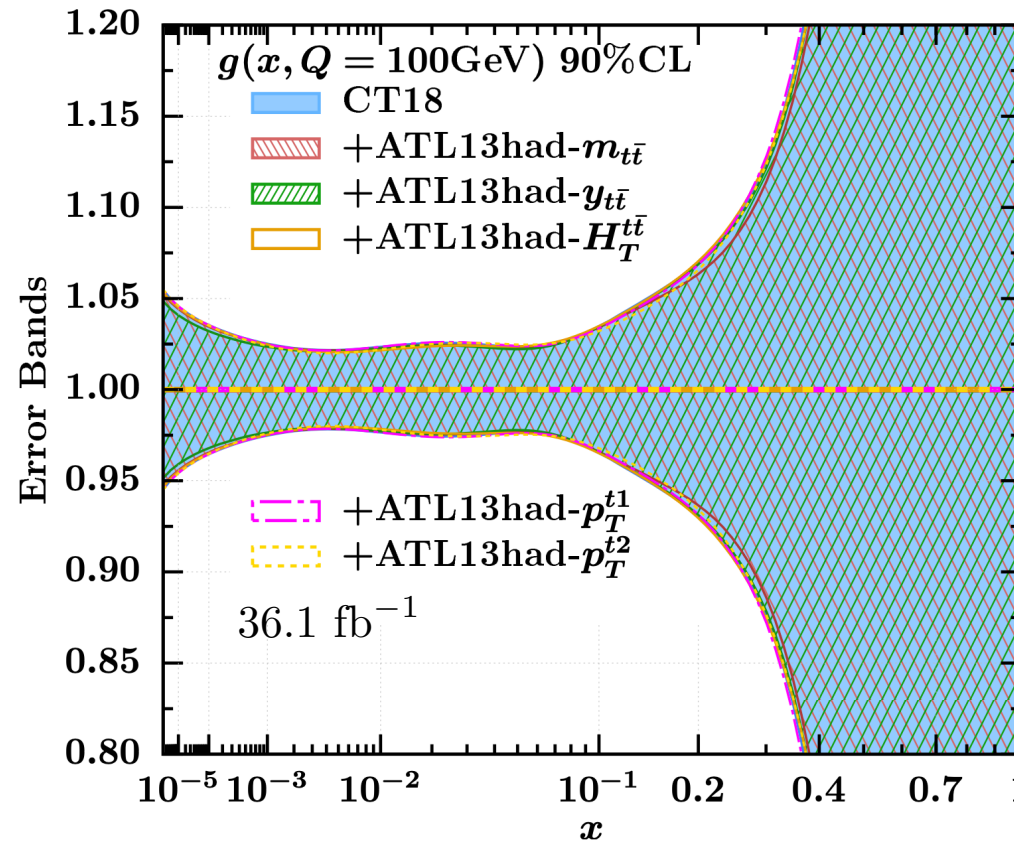
Impact of statistical correlations in ATLAS lep+jets



| Exp | Obs | Npt | ePump updated Chi2/Npt | | | | Global fit Chi2/Npt | | With statistical corr | |
|---|--|-----|------------------------|-------|-------|--|---------------------|---------|-----------------------|-------|
| | | | HT | HT/2 | HT/4 | | HT/2 | HT/4 | HT/2 | HT/4 |
| ATLAS_LepJ ATLAS Bin NoStatCorrelation | m _{t<bar{t}< sub=""></bar{t}<>} | 9 | 1.551 | 1.123 | 0.94 | | 1.27 | 0.92206 | 1.287 | 0.963 |
| | y _{t<bar{t}< sub=""></bar{t}<>} | 7 | 0.911 | 0.739 | 0.8 | | 0.756 | 0.8975 | 0.751 | 0.921 |
| | y _B | 9 | 1.396 | 1.267 | 1.532 | | 0.8498 | 0.93335 | 0.858 | 0.992 |
| | H _{Tt<bar{t}< sub=""></bar{t}<>} | 9 | 1.352 | 0.909 | 0.933 | | 0.805 | 0.80475 | 0.855 | 0.857 |
| | m <sub>t<bar{t}t<bar{t}y<sub>B</bar{t}t<bar{t}y H _{Tt<bar{t}< sub=""></bar{t}<>} | 34 | 1.867 | 1.28 | 1.457 | | 0.933 | 1.06487 | 1.585 | 1.322 |

Some impact on the χ^2/Npt but almost no impact on PDFs and their errors.

Global fit: Impact on $g(x, Q)$ from ATLAS all hadronic

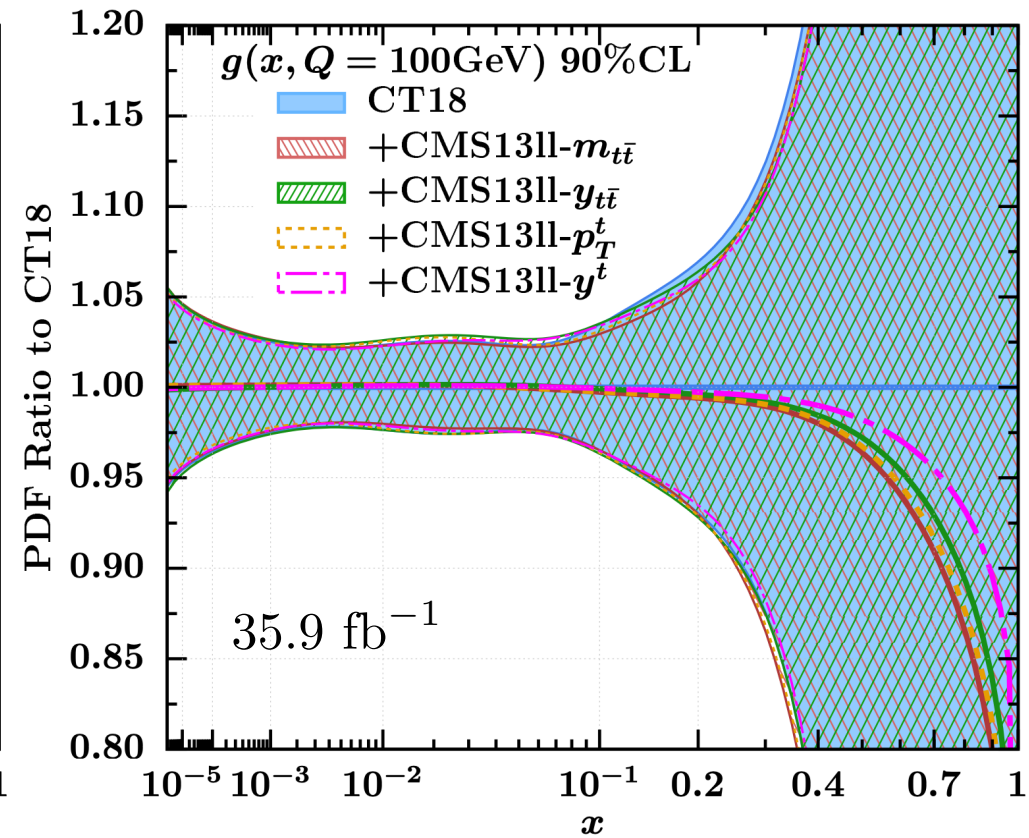
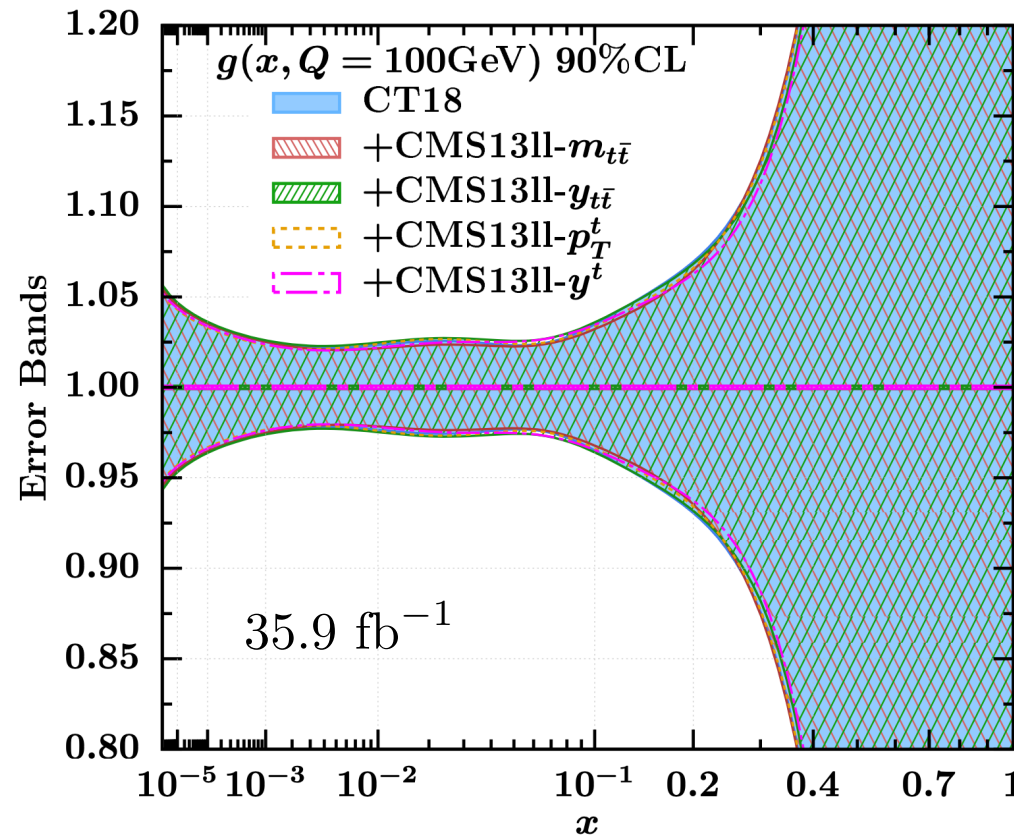


$m_{t\bar{t}}$, $p_{T,t1}$, $p_{T,t2}$, H_T , and $y_{t\bar{t}}$ 1D absolute distributions added one by one in the global fit.

Pulls are in the same direction here.

Impact is very small and confined in the extrapolation PDF parametrization region.

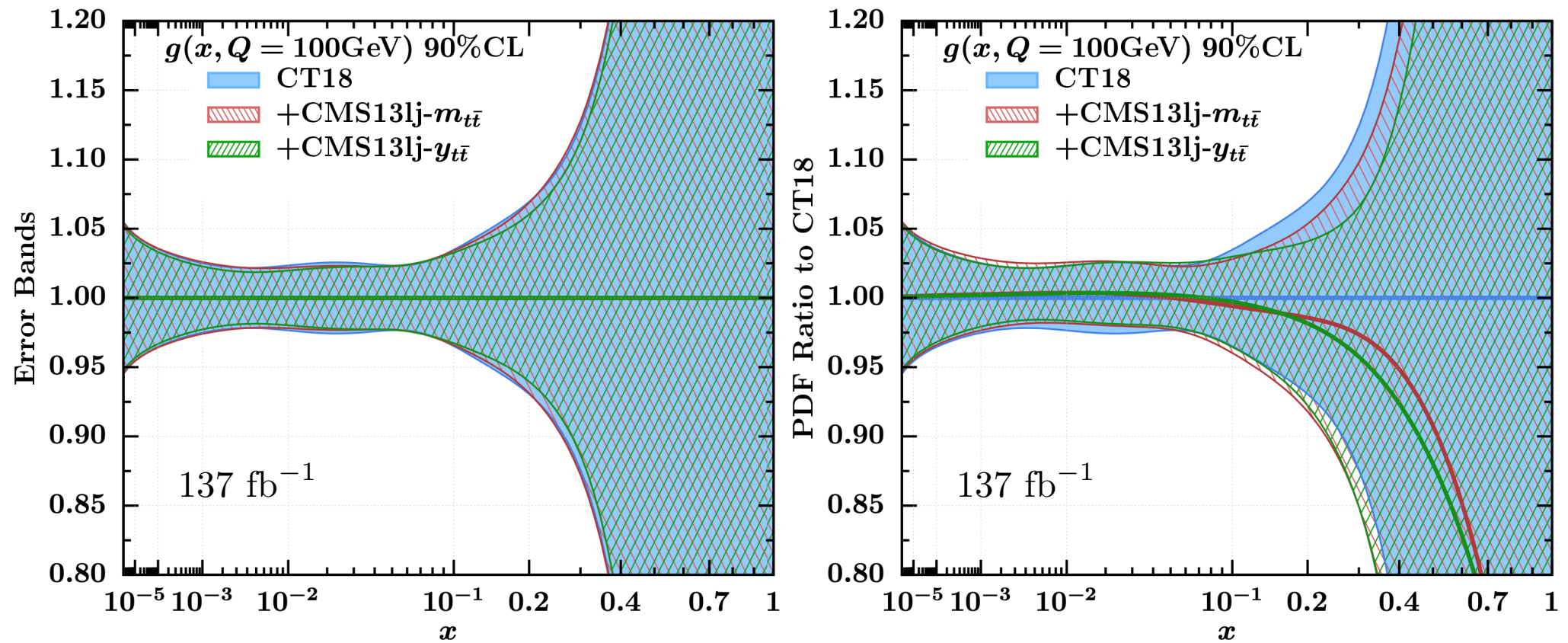
Global fit: Impact on $g(x, Q)$ from CMS dilep



$m_{t\bar{t}}$, p_T , $y_{t\bar{t}}$, and y_t 1D absolute distributions added one by one in the global fit

Pulls are in the same direction here. Moderate impact

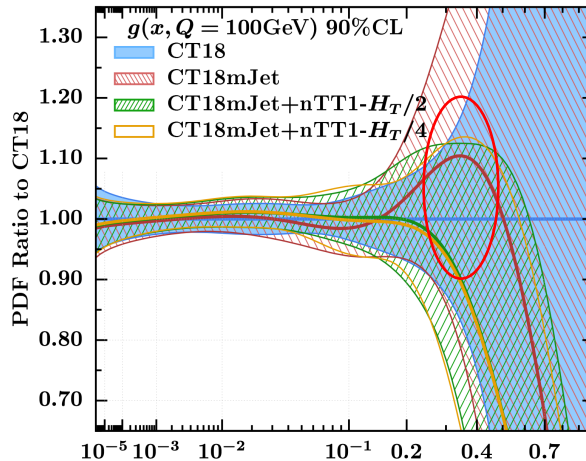
Global fit: Impact on $g(x, Q)$ from CMS lep+jets



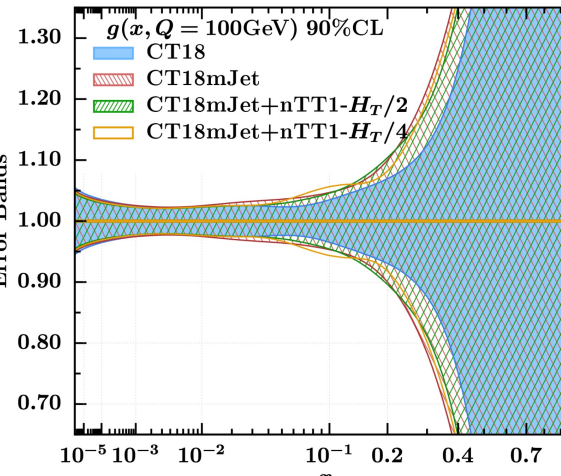
$m_{t\bar{t}}$, and $y_{t\bar{t}}$ 1D absolute distributions added one by one in the global fit

Pulls are in the same direction here: stronger impact due to the higher precision of these data

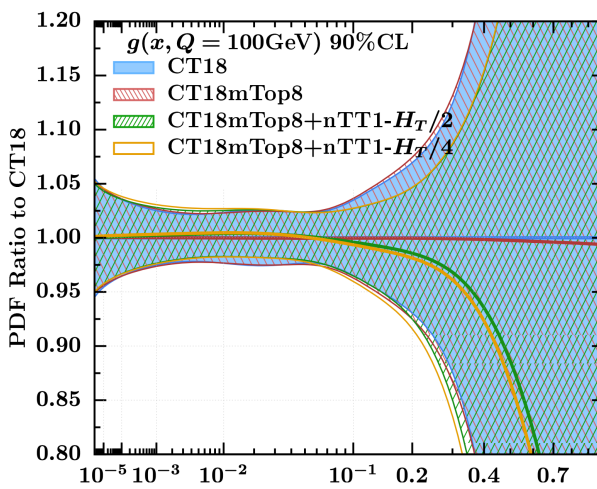
Interplay between top-quark and jet data in CT2X



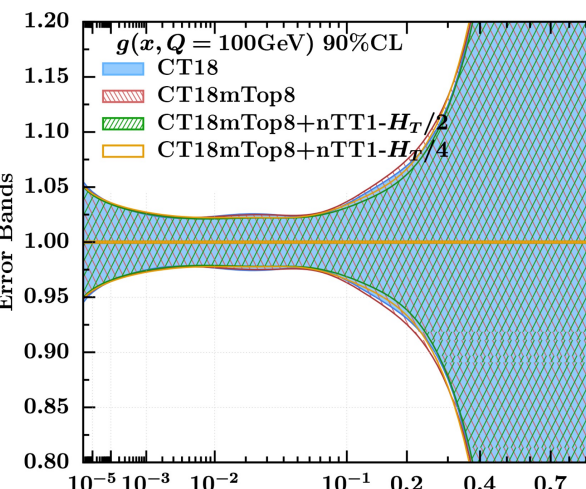
Global fit without jet data vs CT18NNLO



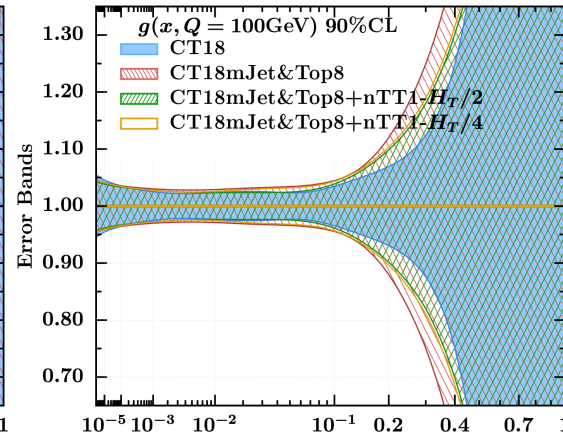
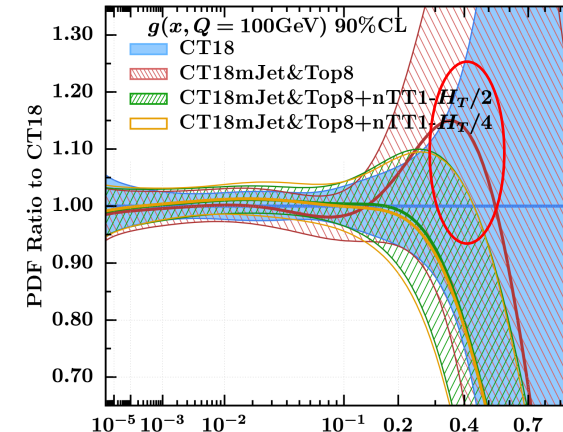
- CT18mTop = CT18 without all ttbar 8 TeV and 13 TeV
- CT18mJet = CT18 without all jet data
- CT18mJet+nTT1-HT/2(4) = CT18 without all jet data but with ttbar 13 TeV (HT/2(4) central scale)
- CT18mTop+nTT1-HT/2(4) = CT18 without all ttbar 8 TeV but with ttbar 13 TeV (HT/2(4) central scale)



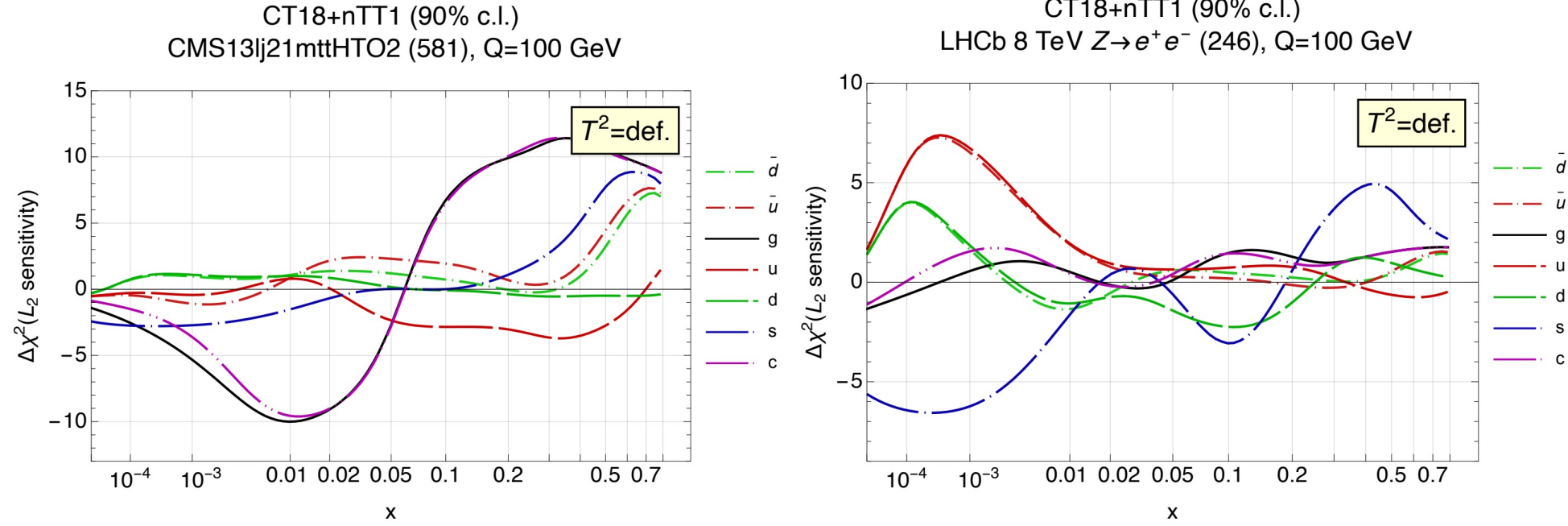
Global fit without $t\bar{t}$ data vs CT18NNLO



Global fit without jet and $t\bar{t}$ data vs CT18NNLO



L2-Sensitivity study of optimal baselines



| ID# | Experimental data set | N_{pt} | $H_T/2$ | | | | $H_T/4$ | | | |
|-----|---|----------|---------|------|------|------|---------|------|------|--|
| | | | CT18 | nTT1 | nTT2 | nTT1 | nTT2 | nTT1 | nTT2 | |
| 110 | CCFR F_2^p | [197] | 69 | 1.1 | 1.1 | 1.1 | 1.2 | 1.2 | 1.2 | |
| 246 | LHCb 8 TeV $2.0 \text{ fb}^{-1} Z \rightarrow e^- e^+$ forward rapidity cross sec. | [193] | 17 | 1.0 | 1.5 | 1.5 | 1.5 | 1.5 | 1.5 | |
| 250 | LHCb 8 TeV $2.0 \text{ fb}^{-1} W/Z$ cross sec. | [194] | 34 | 2.1 | 2.2 | 2.2 | 2.2 | 2.2 | 2.2 | |
| 545 | CMS 8 TeV 19.7 fb^{-1} , single incl. jet cross sec., $R = 0.7$, (extended in y) | [195] | 185 | 1.1 | 1.2 | 1.2 | 1.2 | 1.2 | 1.2 | |
| 573 | CMS 8 TeV 19.7 fb^{-1} , $t\bar{t}$ norm. double-diff. top p_T and y cross sec. | [20] | 16 | 1.2 | 1.2 | 1.2 | 1.1 | 1.1 | 1.1 | |
| 580 | ATLAS 8 TeV 20.3 fb^{-1} , $t\bar{t}$ $p_{T,t}$ and $m_{t\bar{t}}$ abs. spectrum | [17] | 15 | 0.6 | 0.7 | 0.7 | 0.7 | 0.7 | 0.7 | |
| 521 | ATLAS 13 TeV 36.1 fb^{-1} , $t\bar{t}$ abs. $y_{t\bar{t}}$ cross sec. all-hadronic | [22] | 12 | - | 1.0 | 1.0 | 1.1 | 1.1 | 1.1 | |
| 528 | CMS 13 TeV 35.9 fb^{-1} , $t\bar{t}$ abs. $y_{t\bar{t}}$ cross sec. dilepton ch. | [24] | 10 | - | 0.8 | 0.8 | 0.5 | 0.7 | - | |
| 532 | ATLAS 13 TeV 36 fb^{-1} , $t\bar{t}$ abs. $y_{t\bar{t}}$ cross sec. 1+j ch. cms-bin | [21] | 10 | - | 0.7 | - | 0.8 | - | - | |
| 587 | ATLAS 13 TeV 36 fb^{-1} , $t\bar{t}$ abs. $y_{t\bar{t}}$, $m_{t\bar{t}}$, $y_{t\bar{t}}^B$, H_T^{tt} cross secs. 1+j ch. | [21] | 34 | - | - | 0.7 | - | 1.1 | - | |
| 581 | CMS 13 TeV 137 fb^{-1} , $t\bar{t}$ abs. $m_{t\bar{t}}$ cross sec. 1+j ch. | [26] | 15 | - | 1.1 | 1.1 | 1.6 | 1.7 | - | |

Data sets of the extended NNLO global QCD analysis including the optimal combinations CT18+nTT1 and CT18+nTT2. Here we directly compare the quality-of-fit found for CT18+nTT1 and CT18+nTT2 vs. CT18 NNLO

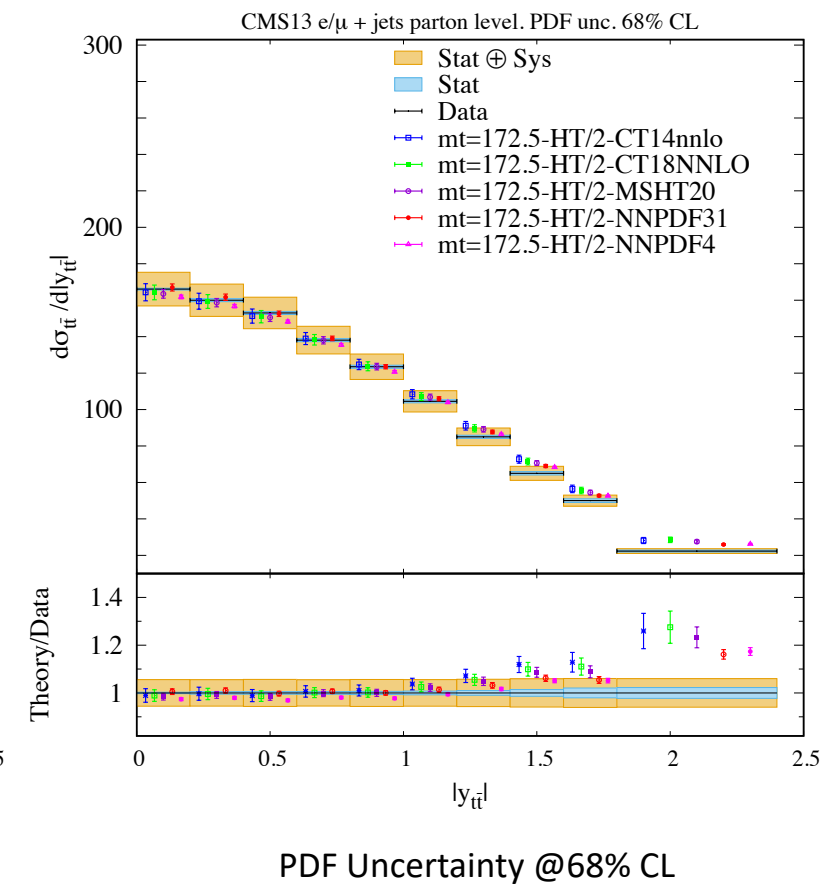
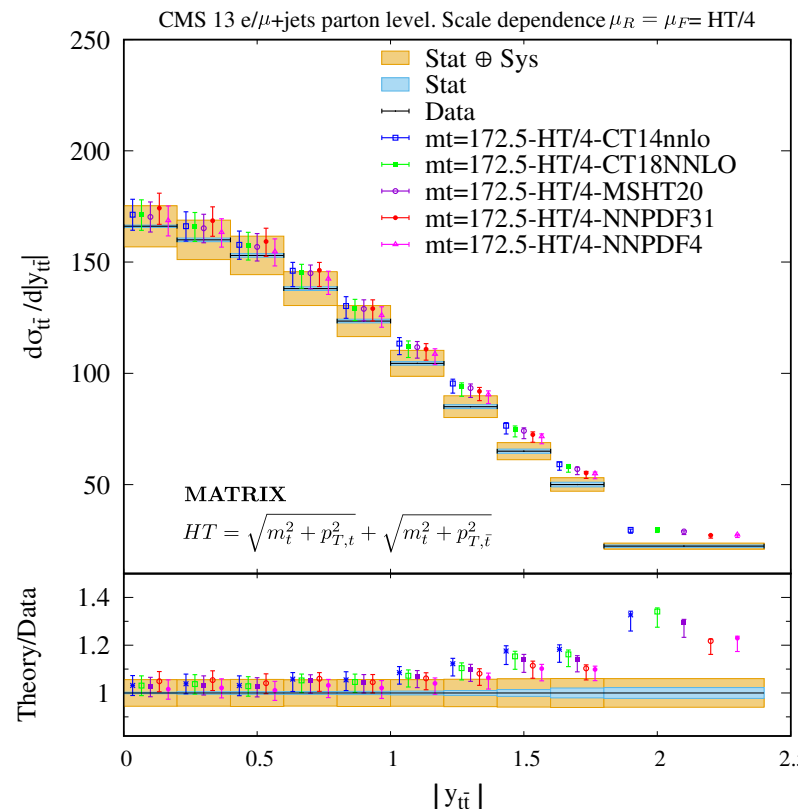
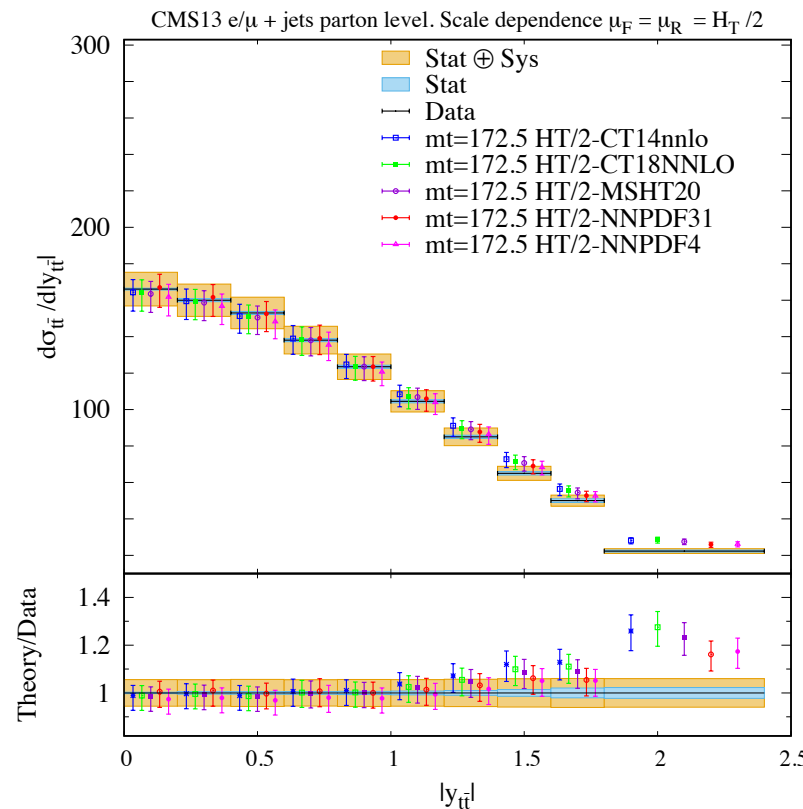
Messages from the ttbar 13 TeV analysis

- First comprehensive study on the impact of LHC 13TeV ttbar data on CT PDFs
- Most of the impact: high-precision data from CMSI+j 13 TeV 137 fb⁻¹
- Pulls on the gluon not in the same direction for some distr. in ATLAS
- Scale uncertainty: the recommended scale choice is not always the best
- Interplay between jets and ttbar: jets still place stronger constraints on $g(x)$
- Optimal baseline for CT2X: ATLAS hadronic: ytt absolute, CMS dilepton: ytt absolute, ATLAS lep+jet: ytt, CMS lep+jet: mtt absolute.
- ttbar 13 TeV data prefer a softer gluon at large x, similar to the LHC jet data.

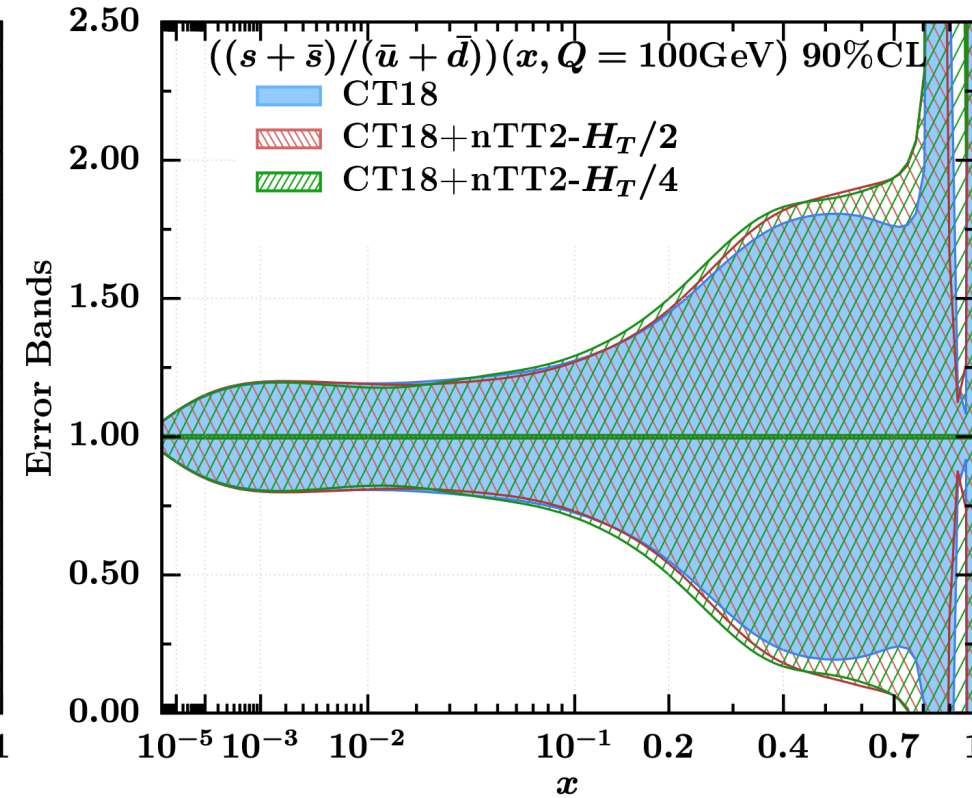
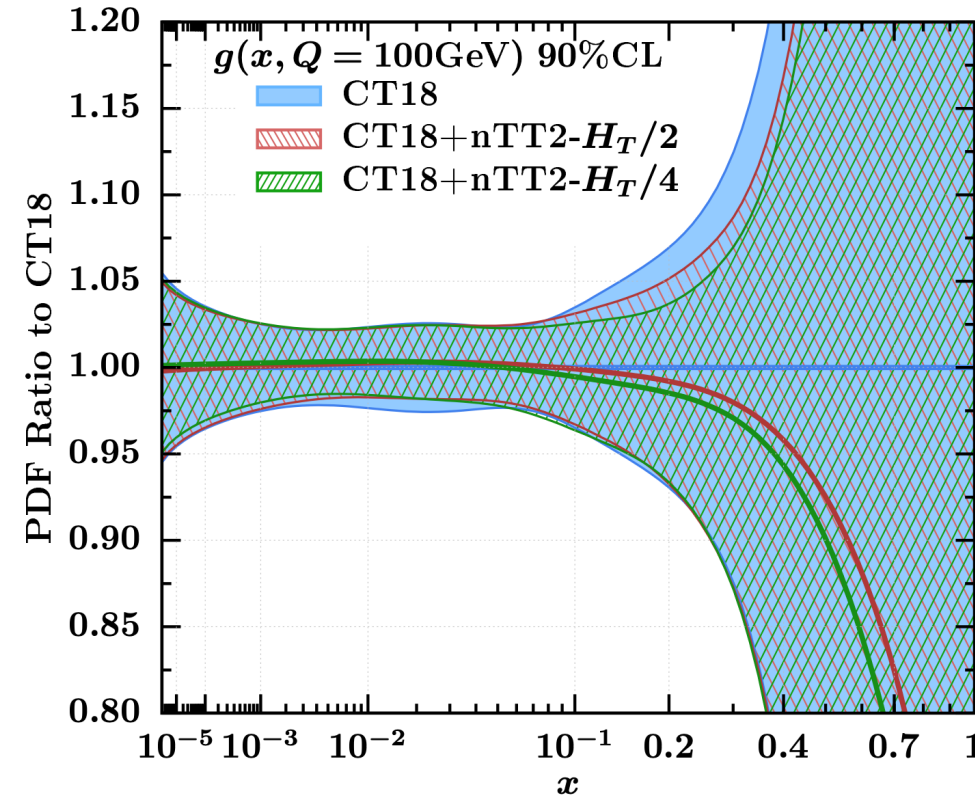
BACK UP

Theory errors: scale choice

Scale uncertainty: the recommended scale choice is not always the best. We select the scale choice that yields the smaller χ^2/N_{pt}



Global fit: impact from new nTT2 baseline



The CT18 analysis

New CTEQ global analysis of quantum chromodynamics with high-precision data from the LHC

Tie-Jiun Hou,^{1,†} Jun Gao,² T. J. Hobbs,^{3,4} Keping Xie,^{3,5} Sayipjamal Dulat,^{6,‡} Marco Guzzi,⁷ Joey Huston,⁸ Pavel Nadolsky,^{9,§} Jon Pumplin,^{8,*} Carl Schmidt,⁸ Ibrahim Sitiwaldi,⁶ Daniel Stump,⁸ and C.-P. Yuan^{8,||}

TABLE I. Datasets included in the CT18(Z) NNLO global analyses. Here we directly compare the quality of fit found for CT18 NNLO vs CT18Z NNLO on the basis of χ_E^2 , $\chi_E^2/N_{pt,E}$, and S_E , in which $N_{pt,E}$, χ_E^2 are the number of points and value of χ^2 for experiment E at the global minimum. S_E is the effective Gaussian parameter [38,42,56] quantifying agreement with each experiment. The ATLAS 7 TeV 35 pb⁻¹ W/Z dataset, marked by ‡, is replaced by the updated one (4.6 fb⁻¹) in the CT18A and CT18Z fits. The CDHSW data, labeled by †, are not included in the CT18Z fit. The numbers in parentheses are for the CT18Z NNLO fit.

| Exp. ID# | Experimental dataset | | $N_{pt,E}$ | χ_E^2 | $\chi_E^2/N_{pt,E}$ | S_E |
|----------|---|------|------------|---------------|---------------------|-------------|
| 160 | HERA I + II 1 fb ⁻¹ , H1 and ZEUS NC and CC $e^\pm p$ reduced cross sec. comb. | [30] | 1120 | 1408 (1378) | 1.3 (1.2) | 5.7 (5.1) |
| 101 | BCDMS F_2^p | [57] | 337 | 374 (384) | 1.1 (1.1) | 1.4 (1.8) |
| 102 | BCDMS F_2^d | [58] | 250 | 280 (287) | 1.1 (1.1) | 1.3 (1.6) |
| 104 | NMC F_2^d/F_2^p | [59] | 123 | 126 (116) | 1.0 (0.9) | 0.2 (-0.4) |
| 108† | CDHSW F_2^p | [60] | 85 | 85.6 (86.8) | 1.0 (1.0) | 0.1 (0.2) |
| 109† | CDHSW $x_B F_3^p$ | [60] | 96 | 86.5 (85.6) | 0.9 (0.9) | -0.7 (-0.7) |
| 110 | CCFR F_2^p | [61] | 69 | 78.8 (76.0) | 1.1 (1.1) | 0.9 (0.6) |
| 111 | CCFR $x_B F_3^p$ | [62] | 86 | 33.8 (31.4) | 0.4 (0.4) | -5.2 (-5.6) |
| 124 | NuTeV $\nu\mu\mu$ SIDIS | [63] | 38 | 18.5 (30.3) | 0.5 (0.8) | -2.7 (-0.9) |
| 125 | NuTeV $\bar{\nu}\mu\mu$ SIDIS | [63] | 33 | 38.5 (56.7) | 1.2 (1.7) | 0.7 (2.5) |
| 126 | CCFR $\nu\mu\mu$ SIDIS | [64] | 40 | 29.9 (35.0) | 0.7 (0.9) | -1.1 (-0.5) |
| 127 | CCFR $\bar{\nu}\mu\mu$ SIDIS | [64] | 38 | 19.8 (18.7) | 0.5 (0.5) | -2.5 (-2.7) |
| 145 | H1 σ_r^p | [65] | 10 | 6.8 (7.0) | 0.7 (0.7) | -0.6 (-0.6) |
| 147 | Combined HERA charm production | [66] | 47 | 58.3 (56.4) | 1.2 (1.2) | 1.1 (1.0) |
| 169 | H1 F_L | [33] | 9 | 17.0 (15.4) | 1.9 (1.7) | 1.7 (1.4) |
| 201 | E605 Drell-Yan process | [67] | 119 | 103.4 (102.4) | 0.9 (0.9) | -1.0 (-1.1) |
| 203 | E866 Drell-Yan process $\sigma_{pd}/(2\sigma_{pp})$ | [68] | 15 | 16.1 (17.9) | 1.1 (1.2) | 0.3 (0.6) |
| 204 | E866 Drell-Yan process $Q^3 d^2\sigma_{pp}/(dQ dx_F)$ | [69] | 184 | 244 (240) | 1.3 (1.3) | 2.9 (2.7) |
| 225 | CDF run-1 lepton A_{ch} , $p_{T\ell} > 25$ GeV | [70] | 11 | 9.0 (9.3) | 0.8 (0.8) | -0.3 (-0.2) |
| 227 | CDF run-2 electron A_{ch} , $p_{T\ell} > 25$ GeV | [71] | 11 | 13.5 (13.4) | 1.2 (1.2) | 0.6 (0.6) |
| 234 | DØ run-2 muon A_{ch} , $p_{T\ell} > 20$ GeV | [72] | 9 | 9.1 (9.0) | 1.0 (1.0) | 0.2 (0.1) |
| 260 | DØ run-2 Z rapidity | [73] | 28 | 16.9 (18.7) | 0.6 (0.7) | -1.7 (-1.3) |
| 261 | CDF run-2 Z rapidity | [74] | 29 | 48.7 (61.1) | 1.7 (2.1) | 2.2 (3.3) |
| 266 | CMS 7 TeV 4.7 fb ⁻¹ , muon A_{ch} , $p_{T\ell} > 35$ GeV | [75] | 11 | 7.9 (12.2) | 0.7 (1.1) | -0.6 (0.4) |
| 267 | CMS 7 TeV 840 pb ⁻¹ , electron A_{ch} , $p_{T\ell} > 35$ GeV | [76] | 11 | 4.6 (5.5) | 0.4 (0.5) | -1.6 (-1.3) |
| 268‡ | ATLAS 7 TeV 35 pb ⁻¹ W/Z cross sec., A_{ch} | [77] | 41 | 44.4 (50.6) | 1.1 (1.2) | 0.4 (1.1) |
| 281 | DØ run-2 9.7 fb ⁻¹ electron A_{ch} , $p_{T\ell} > 25$ GeV | [78] | 13 | 22.8 (20.5) | 1.8 (1.6) | 1.7 (1.4) |
| 504 | CDF run-2 inclusive jet production | [79] | 72 | 122 (117) | 1.7 (1.6) | 3.5 (3.2) |
| 514 | DØ run-2 inclusive jet production | [80] | 110 | 113.8 (115.2) | 1.0 (1.0) | 0.3 (0.4) |

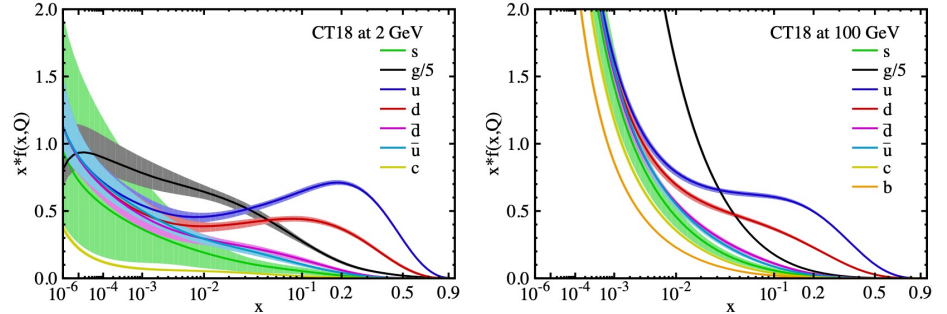


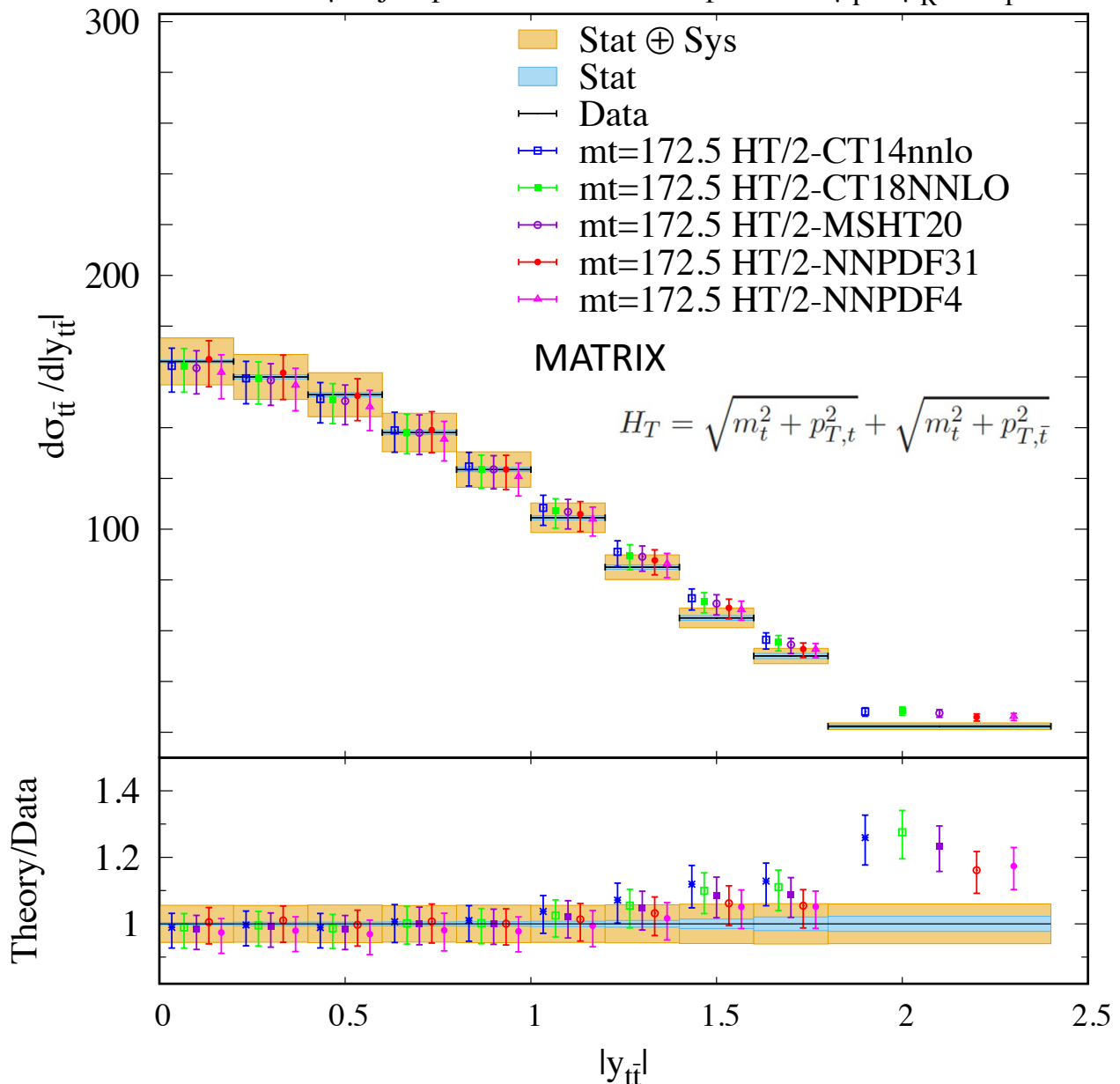
TABLE II. Like Table I, for newly included LHC measurements. The ATLAS 7 TeV W/Z data (4.6 fb⁻¹), labeled by ‡, are included in the CT18A and CT18Z global fits, but not in CT18 and CT18Z.

| Exp. ID# | Experimental dataset | | $N_{pt,E}$ | χ_E^2 | $\chi_E^2/N_{pt,E}$ | S_E |
|----------|---|------|------------|---------------|---------------------|-------------|
| 245 | LHCb 7 TeV 1.0 fb ⁻¹ W/Z forward rapidity cross sec. | [81] | 33 | 53.8 (39.9) | 1.6 (1.2) | 2.2 (0.9) |
| 246 | LHCb 8 TeV 2.0 fb ⁻¹ $Z \rightarrow e^-e^+$ forward rapidity cross sec. | [82] | 17 | 17.7 (18.0) | 1.0 (1.1) | 0.2 (0.3) |
| 248‡ | ATLAS 7 TeV 4.6 fb ⁻¹ , W/Z combined cross sec. | [39] | 34 | 287.3 (88.7) | 8.4 (2.6) | 13.7 (4.8) |
| 249 | CMS 8 TeV 18.8 fb ⁻¹ muon charge asymmetry A_{ch} | [83] | 11 | 11.4 (12.1) | 1.0 (1.1) | 0.2 (0.4) |
| 250 | LHCb 8 TeV 2.0 fb ⁻¹ W/Z cross sec. | [84] | 34 | 73.7 (59.4) | 2.1 (1.7) | 3.7 (2.6) |
| 253 | ATLAS 8 TeV 20.3 fb ⁻¹ , Z p_T cross sec. | [85] | 27 | 30.2 (28.3) | 1.1 (1.0) | 0.5 (0.3) |
| 542 | CMS 7 TeV 5 fb ⁻¹ , single incl. jet cross sec., $R = 0.7$ (extended in y) | [86] | 158 | 194.7 (188.6) | 1.2 (1.2) | 2.0 (1.7) |
| 544 | ATLAS 7 TeV 4.5 fb ⁻¹ , single incl. jet cross sec., $R = 0.6$ | [9] | 140 | 202.7 (203.0) | 1.4 (1.5) | 3.3 (3.4) |
| 545 | CMS 8 TeV 19.7 fb ⁻¹ , single incl. jet cross sec., $R = 0.7$, (extended in y) | [87] | 185 | 210.3 (207.6) | 1.1 (1.1) | 1.3 (1.2) |
| 573 | CMS 8 TeV 19.7 fb ⁻¹ , $t\bar{t}$ norm. double-diff. top p_T and y cross sec. | [88] | 16 | 18.9 (19.1) | 1.2 (1.2) | 0.6 (0.6) |
| 580 | ATLAS 8 TeV 20.3 fb ⁻¹ , $t\bar{t}$ p_T^t and $m_{t\bar{t}}$ abs. spectrum | [89] | 15 | 9.4 (10.7) | 0.6 (0.7) | -1.1 (-0.8) |

Heavy-flavor production measurements at HERA and LHC included in the CT18 NNLO QCD global analysis.

Top-quark pair production diff. Xsec. measurements at 8TeV

CMS13 e/ μ + jets parton level. Scale dependence $\mu_F = \mu_R = H_T / 2$



SCALE DEPENDENCE: HT/2 varied up and down by a factor of 2

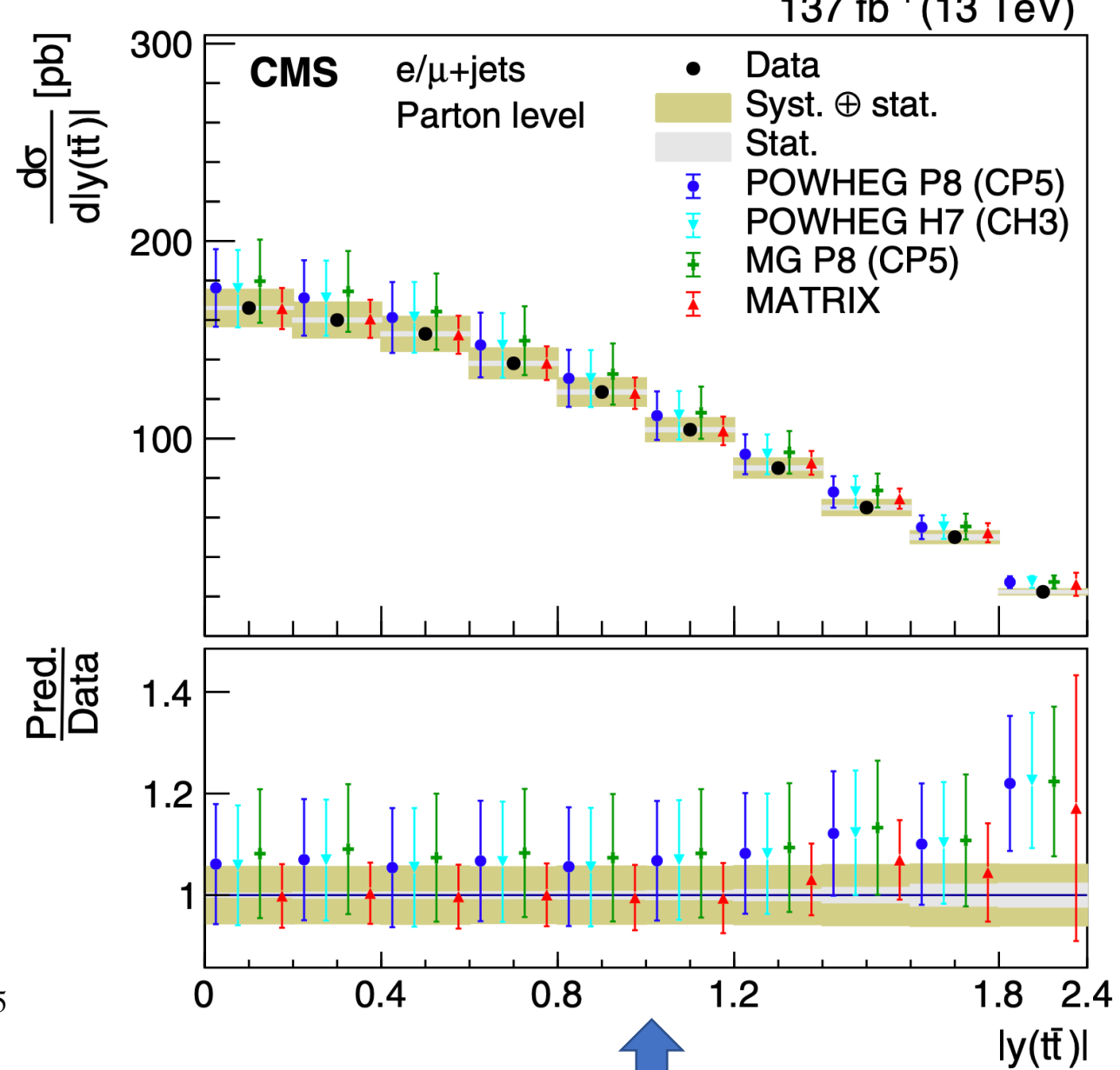
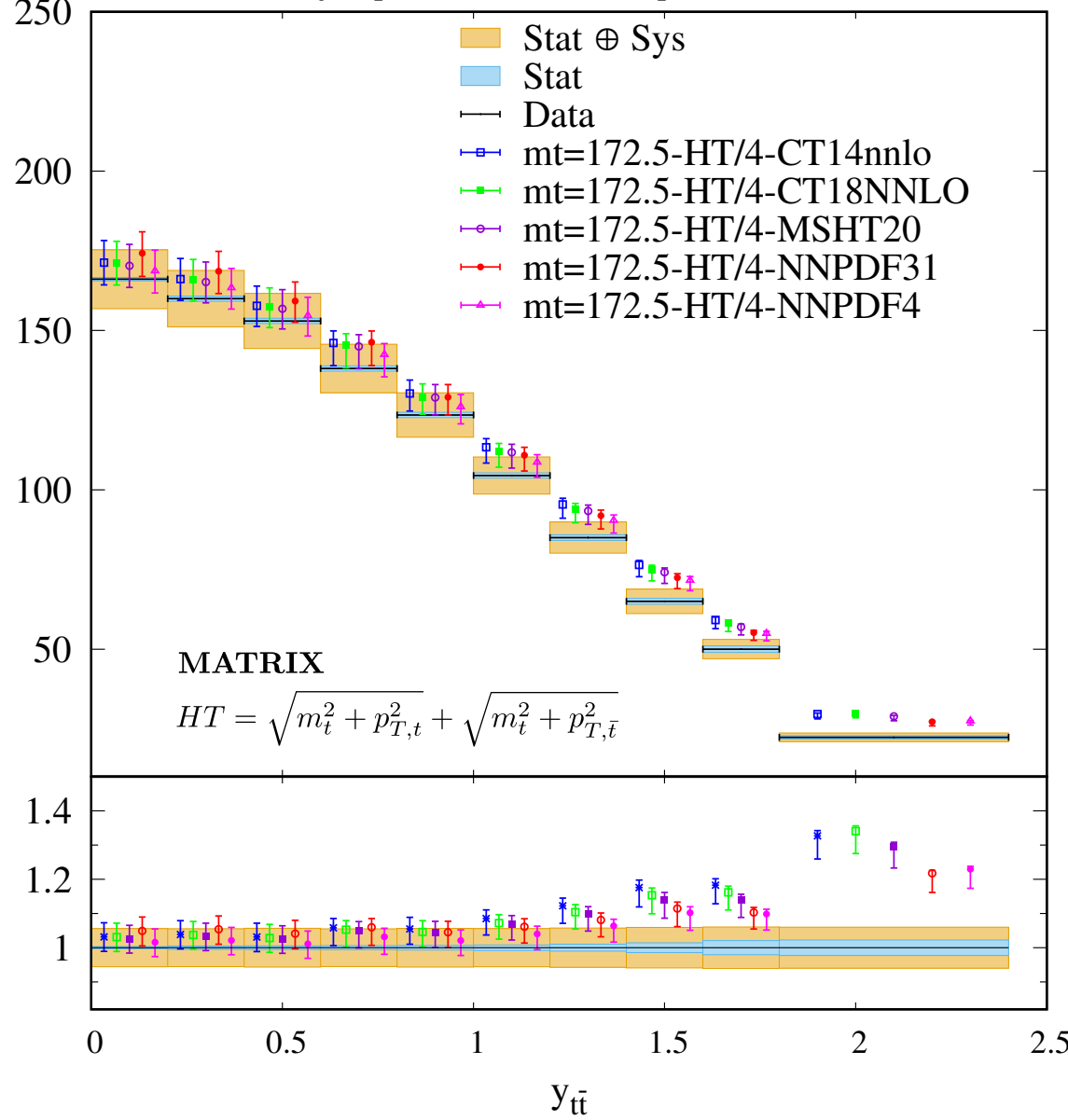


Figure from CMS publication, arXiv:2108.02803
Error: all PDF + scale

CMS 13 e/ μ +jets parton level. Scale dependence $\mu_R = \mu_F = HT/4$



SCALE DEPENDENCE: HT/4 varied up and down by a factor of 2

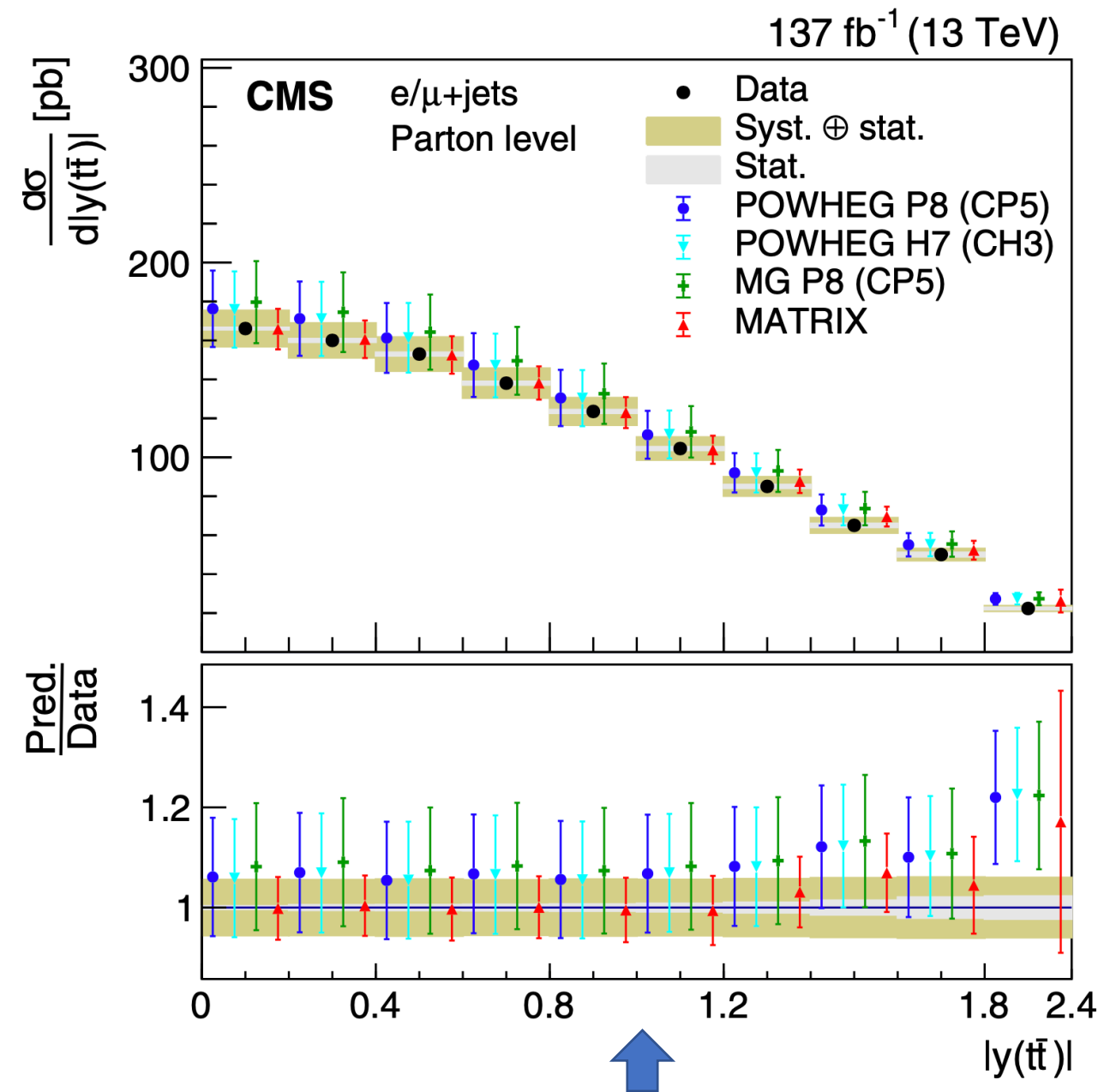


Figure from CMS publication, arXiv:2108.02803
Error: all PDF + scale

